Tracking Performance Analysis and Control of a Small Robotic Telescope System

Thomas Riel, Rudolf Saathof, Andelko Katalenic and Georg Schitter
Automation and Control Institute (ACIN), Vienna University of Technology
Gusshausstrasse 27-29, 1040 Vienna, Austria

ABSTRACT

This paper analyses the achievable precision of an equatorially mounted telescope system with two direct-drive permanent magnet synchronous motors. The analysis is done using a combination of physical system modeling and dynamic error budgeting. The parameters of the physical system are obtained by system identification and parameter estimation for various telescope positions. Using this system model, the limiting performance of the telescope system is simulated. Based on the identification data, a feedback controller is designed and implemented for the telescope system. The performance is verified experimentally by measurements recorded at tracking speeds of up to 5 °/s and several positions. The experimental results reveal a maximal servo tracking error of 1.3 arcseconds for the dec.-axis and 0.5 arcseconds for the r.a.-axis, which occurs at the maximal speed of 5 °/s. The experimental results are in good agreement with the simulation results, verifying the proposed method. This method provides a powerful tool to compare various systems by simulation as well as to optimize the performance of robotic telescope systems for tracking of NEOs to improve space situation awareness.

1. INTRODUCTION

Optical ground stations (OGSs) for satellite laser ranging (SLR) and optical surveillance are an integral part of many space situation awareness programs. Large networks of robotic telescopes are key for achieving a good coverage and monitoring [1]. SLR systems work by transmitting short laser pulses from the OGSs to the measured object in orbit. The light is reflected by the object and detected by the OGS. The travel time is measured and converted to a distance, thus together with the known telescope pose, defines the position of the object. To increase the reflected energy, strong laser beams with a very small divergence angle are required [2]. The same requirements also apply for other applications, e.g. optical satellite communication [3]. As the intensity of a gaussian beam is concentrated in the center, a precise tracking of the satellite trajectory with a servo precision of one tenth of the beam divergence is typically required, even at high telescope velocities [3]. The design of a high performance telescope system used for SLR in Korea is described in literature [4]. The servo precision of the system is reported to be mostly below 0.3 arcseconds, with a worst case error of 1.67 arcseconds for a representative trajectory of the ISS [5]. The used trajectory shows a maximum velocity of 8 °/s. For a representative trajectory of the GOCE satellite the error in the elevation and azimuth axes are below 0.3 arcseconds and 0.1 arcseconds, respectively. The maximum velocity for this trajectory is below 0.2 °/s for the elevation and below 1 °/s for the azimuth axis. Commercial off the shelf telescopes often lack this level of precision, particularly at high speeds.

To achieve precise motion with errors in the sub-arcsecond range, a detailed analysis of the present disturbance sources and good mechatronic design of the system are necessary. In this paper, the effects of stochastic disturbances acting in the drive system of an equatorial telescope system are analyzed. If not considered in the system design, these disturbances fundamentally limit the achievable precision of a telescope system. The analysis is done by dynamic error budgeting (DEB), using power spectral densities (PSDs) of the noise sources, as described by [6].
The analyzed telescope system incorporates of two direct-drive permanent magnet synchronous motors (PMSM) and precise optical encoders with milliarcsecond resolution. Direct-drive PMSMs are widely used in servo systems for precision positioning applications, e.g. robots [7] or telescope systems [5] [8] [9]. They offer the advantage of high power density and high dynamic performance [10] and show no backlash.
The analysis is used to determine the limiting performance of the investigated system. Based on system identification, a controller is designed for the used telescope system. The simulated performance of the system is then compared to experiments.

The remainder of this paper is organized as follows. Section 2 starts with the description of the analyzed system, which is mathematically modeled in Section 3. The performance simulation is presented in Section 4. The model is then

identified and utilized in Section 5 to design a suitable controller for the system. A short overview of the implementation of the control system is given in Section 6. Section 7 present the experimental validation of the performance. Finally, the conclusion is given in Section 8.

2. SYSTEM DESCRIPTION

An equatorial telescope system with direct-drive PMSMs is used as basis for the analysis. The used telescope mount incorporates two PMSMs with 11 pole pairs and a rated torque of 6.44 Nm and 13.96 Nm in the declination (dec.) and right ascension (r.a.) axis. The used telescope is a mock up with a diameter of 12 inch and includes aluminum weights to simulate the mass of the primary and secondary mirror. The system is mounted on a wooden tripod. An illustration of the used system is shown in Fig. 1. Similar systems are in active use for SLR and space debris observation [11].

The telescope mount uses one optical encoders per axis to detect the motion of the axis. A custom made switched amplifier with 100 kHz switching frequency is used to drive the two PMSMs. Hall sensors are used to measure the individual phase currents of the PMSMs.

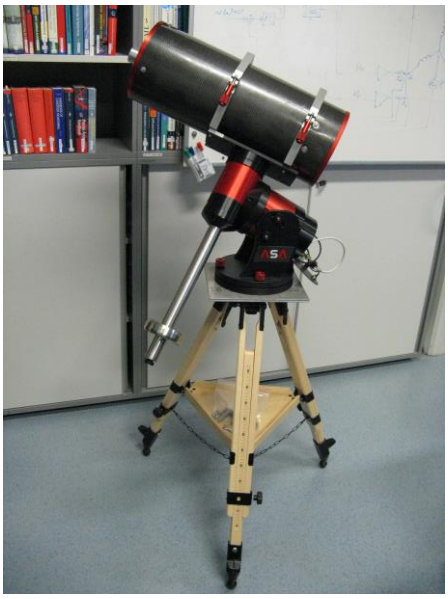

Fig. 1: Used equatorial telescope system with direct-drive telescope mount and 12" telescope mock-up.

3. SYSTEM MODELING

To model the behavior of the telescope system, a mathematic description of the two axis telescope mount is used. A schematic overview of the drive and control system of an individual axis of the telescope mount is given in Fig. 2. To simulate the performance of the system, a linear time-invariant model of every component is derived.

PMSM

The direct-drive PMSM of an individual axis is modeled using an electro-mechanical model as described by [12]. The electro-mechanical model uses the Park transformation [13] to describe the motor in rotor coordinates. As the individual axis are assumed to be well balanced, the main disturbance acting on the drive system is the friction torque. The friction is assumed to be purely viscous friction [14], described by the parameter β. The electro-mechanical description of a single axis is then given by

$$\frac{d\varphi}{dt} = \omega \tag{1}$$

$$\frac{d\omega}{dt} = \frac{1}{J}\left(K_m i_q - \beta\omega\right) \tag{2}$$

$$\frac{di_d}{dt} = \frac{1}{L_d}\left(u_d - Ri_d + L_q i_q Z_p \omega\right) \tag{3}$$

$$\frac{di_q}{dt} = \frac{1}{L_q}\left(u_q - Ri_q - \Psi_M Z_p \omega + L_d i_d Z_p \omega\right) \tag{4}$$

where φ is the axis angle, ω is the angular velocity, J is the moment of inertia, K_m is the torque constant, Z_p is the number of pole pairs, Ψ_M is the mutual flux due to the magnets, R is the phase resistance, i_q and i_d are the current in the quadrature and direct axis (q and d-axis), L_q and L_d are the inductances of the q- and d-axis and u_q and u_d are the voltages applied to the q- and d-axis.

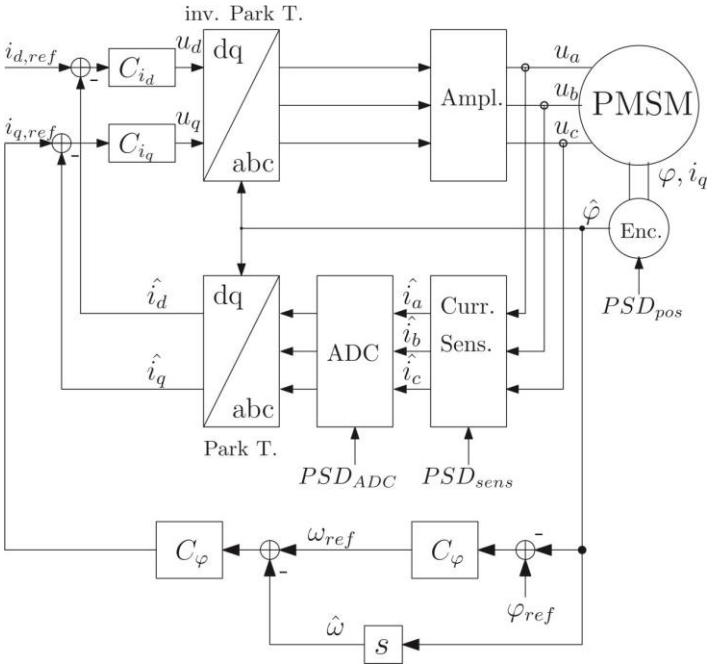

Fig. 2: Schematic representation of a single PMSM axis.

PMSM driver and position sensor:

Due to the much faster dynamic response (10 kHz and higher) of the current sensors, ADC, optical angular encoder and the amplifier, they are modeled by constant amplification factors. The noise of the three phase current sensors, the optical angular encoder and the three ADCs are modeled by their PSD. All noise sources are assumed to be white gaussian noise. The influence of the PWM signal is neglected in this analysis, as the switching frequency is two orders of magnitude higher than any relevant system dynamics and therefore well attenuated.

Control system:
As is common for PMSMs [10], the control system for an individual axis consists of a cascade of PI controllers: two PI controllers are used to control the d and q-component of the current, one PI controller is utilized for the inner velocity control loop and finally a PI controller is added for position control of the axis. This cascaded control structure is also visible in Fig. 2.

The necessary model parameters are extracted from the data sheets or identified using measurements. A list of the used model parameters is given in Tab. 1.

Tab. 1: System parameters used for simulation.

Parameter	**Dec-axis**	**R.a.-axis**
Inertia J	0.19 kg m²	2.2 kg m²
Viscosity β	1.3 Nm/rad/s	7.8 Nm/rad/s
Number of pole pairs Z_p	11	11
Resistance R	1.31 Ω	1.02 Ω
Inductance L_q	3.3 mH	5.45 mH
Inductance L_d	3.9 mH	5.41 mH
Torque constant K_m	1.81 Nm/A	2.43 Nm/A
Current control bandwidth	1.5 kHz	1.5 kHz
Velocity control bandwidth	15 Hz	10 Hz
Position control bandwidth	10 Hz	8 Hz
Current sensor noise	64 µA/√Hz	64 µA/√Hz
Current sensor gain	0.325 V/A	0.325 V/A
Encoder noise	1.2 nrad/√Hz	1.2 nrad/√Hz
Amplifier gain	20	20

4. SIMULATION RESULTS

To simulate the limiting performance of the telescope system, dynamic error budgeting (DEB) is used. DEB allows to estimate performance of a system by modeling the stochastic disturbances acting on the system by their corresponding PSD as described by [6]. The disturbances are propagated through the linear, time-invariant (LTI) models describing the system to determine their effect on the system output. A detailed description of the used simulation method is given in [15]. Also included in [15] is the calculation of the necessary transfer functions of the system.
The resulting PSD of the position noise is visualized as the cumulative power spectral density in Fig. 3. The simulated RMS error of the telescope system is 0.17 arcseconds for the dec.-axis and 0.09 arcseconds for the r.a.-axis. This performance is well within the necessary requirements for SLR. Utilizing a well-designed control system, the analyzed telescope system should be able to be used for satellite tracking applications.

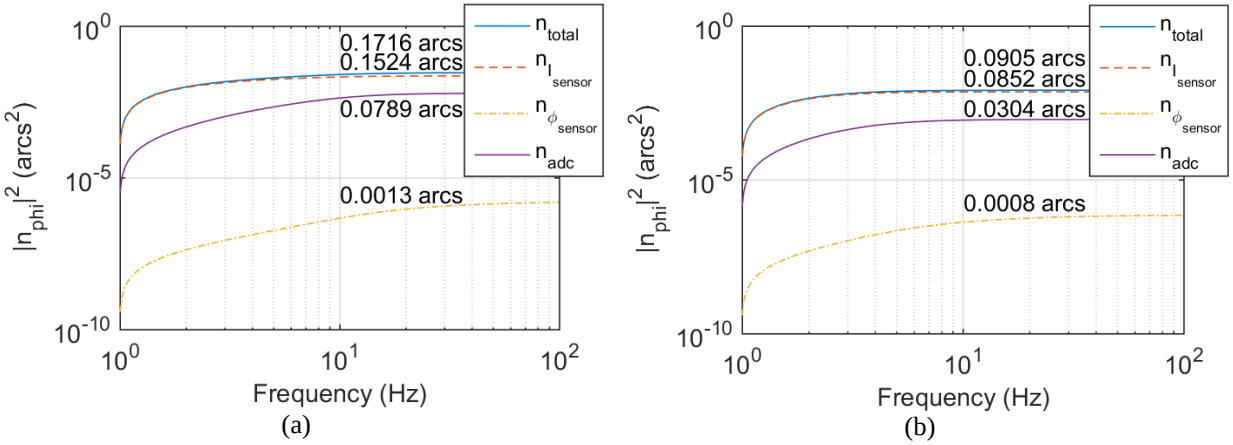

Fig. 3: Cumulative power spectral density of the position noise for the (a) dec-axis and (b) r.a.-axis.

5. IDENTIFICATION AND CONTROL DESIGN

To enable a highly dynamic control of the telescope system, the inner current control loops are tuned for a closed loop bandwidth of 1.5 kHz. The telescope system is then identified using open loop identification experiments with sweped sinusoids. To identify the system dynamics, the open loop transfer function from the i_q-reference to the velocity ω is measured. However, the frequency response varies for different poses of the telescope system. In Fig. 4, the nominal frequency response function is shown, which was constructed from measurements at four different angular positions of each axis. Especially the first anti-resonance/resonance appears to be influenced by the angular position of the telescope system.

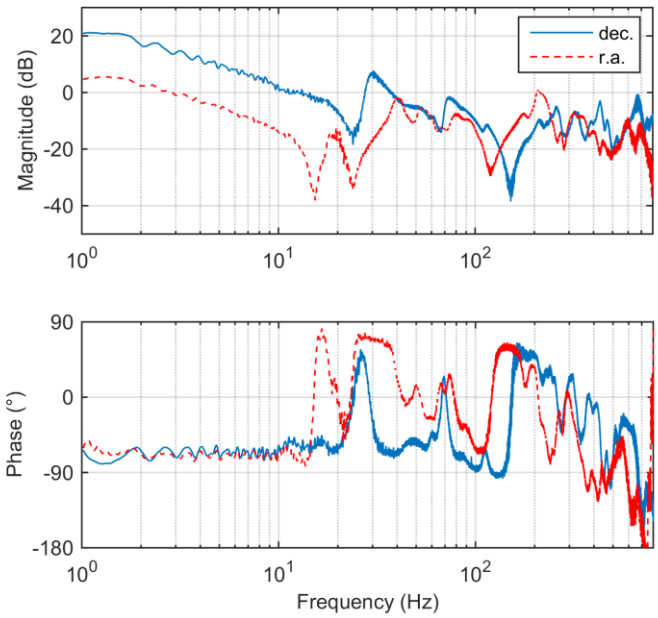

Fig. 4: Nominal open loop frequency response function for the velocity loop of the dec. and r.a.-axis of the telescope system.

Based on the identified dynamics, a controller is designed for the velocity control loop. The identified frequency response for the neutral telescope position is used as nominal plant model. It is visible in Fig. 4 that at 20 Hz in the dec.-axis first structural dynamics, while in the r.a.-axis first structural dynamics occur at 14 Hz. Although, a closed loop control bandwidth above these frequency can be reached, a closed loop bandwidth of 15 Hz for the dec.-axis and 10 Hz for the r.a.-axis is chosen for the control design. Controlling the motion of the axis above this frequency may result in a smaller servo error, but will not necessarily improve the precision of the telescope system itself, as the system may not behave as a rigid body [16].

Dec.-axis controller design:
A notch filter is used to suppress the critical resonance peak in the dec.-axis. In addition to the notch filter, a low-pass filter is used to suppress resonant peaks at high frequency. A PI controller is used to achieve the desired crossover frequency. The resulting complementary sensitivity function of the velocity loop is shown in Fig. 5. The closed loop bandwidth of the position control loop is set to 10 Hz. A PI controller is utilized to reach the desired bandwidth.

R.a.-axis controller design:
A notch filter is used to suppress the critical resonance peak in the r.a.-axis. In addition to the notch filter, a low-pass filter is used to suppress resonant peaks at higher frequency. A PI controller is used to reach the desired crossover frequency. The resulting complementary sensitivity function of the velocity loop is shown in Fig. 5. Unfortunately the phase of the measurements is sensitive to noise and the measurement above 50 Hz is therefore corrupted. The closed loop bandwidth of the position control loop is set to 8 Hz. The used PI controller is tuned to reach the desired closed loop bandwidth.

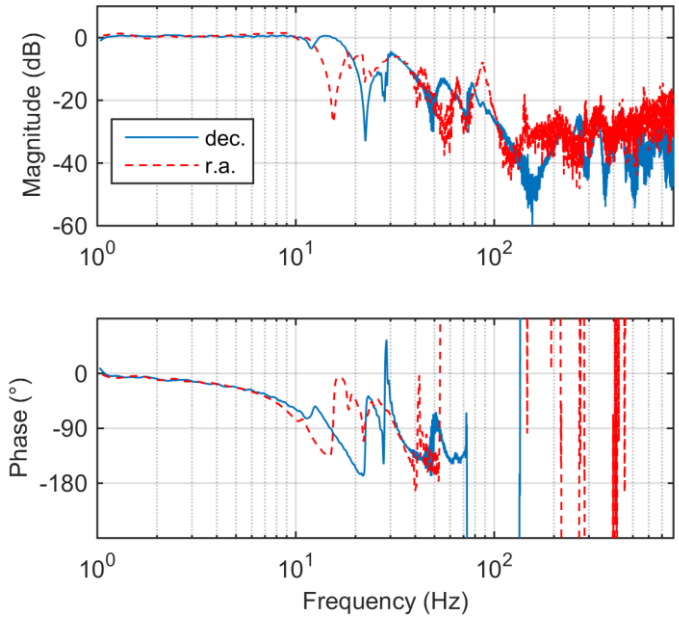

Fig. 5: Complementary sensitivity function of the velocity loop for the dec. and r.a.-axis.

6. IMPLEMENTATION

The entire control system is implemented on a dSpace Rapid Prototyping system (DS1202, dSpace GmbH, Germany). The current control system together with the encoder readout is implemented on the FPGA of the dSpace system. A sampling frequency of 100 kHz is used for the current control. The current measurement is synchronized with the PWM frequency. The velocity as well as the position control are implemented on the processor system of the dSpace. A sampling frequency of 20 kHz is used.

7. EXPERIMENTAL RESULTS

The RMS position error of the telescope servo system is used to measure the performance of the system. As the dynamics of the system change with the velocity as well as the position of the individual axis, these two parameters are varied in the experimental validation of the performance.
The tested velocity range starts at sidereal speed (15 arcseconds/s or 0.0042 °/s) and ends at a maximum velocity of 5 °/s. This maximum velocity would allow to track the ISS up to an elevation of 78° and is therefore considered sufficient for most tracking applications. As the behavior of the telescope system is symmetric around the neutral position, the axis position is only varied over a range of zero to 90°. An automatic measurement procedure is used to measure at 10 variations of each parameter, i.e. 100 data points.

The RMS position error for the dec.-axis as a function of the dec.-axis velocity for three different r.a.-axis position is shown in Fig. 6 a). The position error is independent of the r.a.-axis position and increases with the dec.-axis velocity. The error remains below 0.5 arcseconds up to a velocity of 1 °/s and below 1.3 arcseconds up to the maximum velocity of 5°/s.

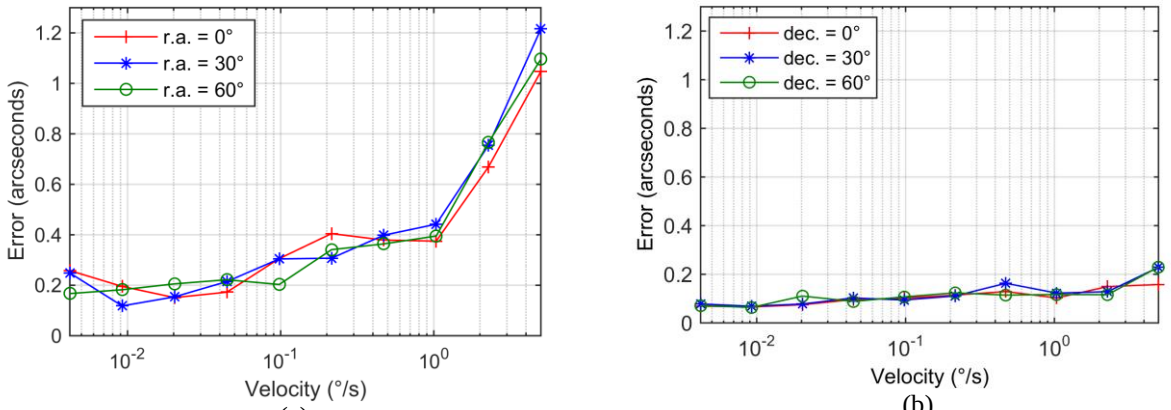

(a) (b)

Fig. 6: RMS position error of the (a) dec.-axis as a function of the dec.-axis velocity and the r.a.-axis position and (b) of the r.a.-axis as a function of the r.a.-axis velocity and the dec.-axis position.

The RMS position error for the r.a.-axis as a function of the r.a.-axis velocity for three different dec.-axis position is shown in Fig. 6 b). The error is independent from the dec-axis position but increases with the r.a.-axis velocity. The error remains below 0.24 arcseconds up to the maximum velocity of 5 °/s and below 0.16 arcseconds up to a velocity of 2.2 °/s.

In summary it can be concluded from the experimental data that the simulated performance is in good agreement with the experimental validation at low velocities. At higher velocity unmodeled dynamics of the mount and the telescope appear to degrade the performance. Nevertheless, the achieved tracking precision is sufficient for the intended application of SLR or optical satellite communication.

8. CONCLUSIONS

This paper presents the simulation and experimental validation of the tracking precision of an equatorial telescope system with a 12 inch telescope. It is verified, that the investigated servo system is able to track the desired trajectory with an error of less than 0.5 arcseconds for velocities of up to 1 °/s and with an error of less than 1.3 arcseconds for velocities from 15 arcseconds/s up to a maximum of 5°/s. Physical models are used to represent the system for the dynamic error budget. The simulation results indicate a limiting precision of the telescope system of 0.17 arcseconds for the dec.-axis and 0.09 arcseconds for the r.a.-axis. Identification of the telescope system at various poses is used to design a robust controller. The control bandwidth is limited by structural dynamics of the system. The performance of the system is validated using 100 data points at different speeds and poses. The performance measurements are in good agreement with the simulation at low velocity. For higher velocities, additional, dynamics of the mount and the telescope start to degrade the tracking performance. Increasing the control bandwidth may reduce these effects, but requires a different mechatronic design of the system.

ACKNOWLEDGEMENTS

This work has been funded by the Austrian research funding association (FFG) under the scope of the Bridge program (contract number 850722) provided by the bmvit.

REFERENCES

[1] M. Laas-Bourez, D. Coward, A. Klotz and M. Boër, "A robotic telescope network for space debris identification and tracking," *Advances in Space Research*, vol. 47, no. 3, pp. 402-410, 2011.

[2] G. Kirchner, F. Koidl, F. Friederich, I. Buske, U. Völker and W. Riede, "Laser measurements to space debris from Graz SLR station," *Advances in Space Research*, vol. 51, no. 1, pp. 21-24, 2013.

[3] H. Hemmati (Ed.), Near-earth laser communications, CRC press, 2009.

[4] J. H. Jo, I. K. Park, H.-C. Lim, Y.-K. Seo, H.-S. Yim, J.-Y. Lee, S.-C. Bang, J. Nah, K. D. Kim, J. G. Jang, B. H. Jang, J. H. Park and J.-U. Park, "The design concept of the first mobile satellite laser ranging system (ARGO-M) in Korea," *Journal of Astronomical Space Science,* vol. 28, no. 1, p. 93–112, 2011.

[5] C. H. Park, Y. S. Son, B. I. Kim, S. Y. Hama, S. W. Lee and H. C. Lim, "Design of tracking mount and controller for mobile satellite laser ranging system," *Advances in Space Research,* vol. 49, p. 177–184, 2012.

[6] L. Jabben and J. van Eijk, "Performance analysis and design of mechatronic systems," *Mikroniek*, pp. 5-12, 2011.

[7] S. Thielmann, U. Seibold, R. Haslinger, G. Passig, T. Bahls, S. Jörg and G. Hirzinger, "Mica-a new generation of versatile instruments in robotic surgery," in *Intelligent Robots and Systems (IROS), 2010 IEEE/RSJ International Conference on*, 2010.

[8] P. Gutierrez, "Standardization of direct drive servos in telescope applications," in *Astronomical Telescopes and Instrumentation. International Society for Optics and Photonics*, 2003.

[9] C. J. Jian, M. W. Li and H. J. & Long, "Design and optimization of arc permanent magnet synchronous motor used on large telescope," *IEEE transactions on magnetics,* vol. 45, no. 5, pp. 1943-1947, 2012.

[10] W. Leonhard, Control of electrical drives, Springer Science & Business Media, 2001.

[11] J. Herzog, T. Schildknecht, A. Hinze, M. Ploner and A. Vananti, "Space Surveillance Observations at the AIUB Zimmerwald Observatory," in *6th European Conference on Space Debris, Proceedings of the conference*, Darmstadt, 2013.

[12] P. Pillay and R. Krishnan, "Modeling, simulation, and analysis of permanent-magnet motor drives. I. The permanent-magnet synchronous motor drive," *IEEE Transactions on industry applications,* vol. 25, no. 2, pp. 265-273, 1989.

[13] R. Park, "Two-reaction theory of synchronous machines generalized method of analysis-part I," *Transactions of the American Institute of Electrical Engineers,* vol. 48, no. 3, pp. 716-726, 1929.

[14] B. Armstrong-Helouvry, Control of machines with friction, Springer Science & Business Media, 2012.

[15] T. Riel, R. Saathof, A. Katalenic and G. Schitter, "Noise Analysis and Improvement of a Permanent Magnet Synchronous Motor by Dynamic Error Budgeting," in *7th IFAC Symposium on Mechatronic Systems*, Loughborough, 2016.

[16] R. M. Schmidt, G. Schitter and A. Rankers, The Design of High Performance Mechatronics-: High-Tech Functionality by Multidisciplinary System Integration, IOS Press, 2014.